PAPER • **OPEN ACCESS**

Evaluation of cardiovascular and cerebrovascular control mechanisms in postural orthostatic tachycardia syndrome via conditional transfer entropy: the impact of the respiratory signal type

To cite this article: Francesca Gelpi *et al* 2023 *Physiol. Meas.* **44** 064001

IOP Publishing Physiol. Meas. 44 (2023) 064001 https://doi.org/10.1088/1361-6579/acdb47

Physiological Measurement

IPEM Institute of Physics and Engineering in Medicine

OPEN ACCESS

RECEIVED
17 January 2023

REVISED
17 May 2023

ACCEPTED FOR PUBLICATION
1 June 2023

PUBLISHED
19 June 2023

PAPER

Evaluation of cardiovascular and cerebrovascular control mechanisms in postural orthostatic tachycardia syndrome via conditional transfer entropy: the impact of the respiratory signal type

Francesca Gelpi[1], Vlasta Bari[1,2], Beatrice Cairo[1], Beatrice De Maria[3], Rachel Wells[4], Mathias Baumert[5] and Alberto Porta[1,2,*]

[1] Department of Biomedical Sciences for Health, University of Milan, Milan, Italy
[2] Department of Cardiothoracic, Vascular Anesthesia and Intensive Care, IRCCS Policlinico San Donato, San Donato Milanese, Milan, Italy
[3] IRCCS Istituti Clinici Scientifici Maugeri, Milan, Italy
[4] Department of Medicine, Royal Adelaide Hospital, Port Road, Adelaide, Australia
[5] Discipline of Biomedical Engineering, School of Electrical and Mechanical Engineering, The University of Adelaide, Adelaide, Australia
[*] Author to whom any correspondence should be addressed.

E-mail: alberto.porta@unimi.it

Keywords: vector autoregresssive model, heart rate variability, cerebral blood flow, baroreflex, cerebral autoregulation, autonomic nervous system, active standing

Abstract

Objective. Closed loop cardiovascular (CV) and cerebrovascular (CBV) variability interactions are assessed via transfer entropy (TE) from systolic arterial pressure (SAP) to heart period (HP) and vice versa and from mean arterial pressure (MAP) to mean cerebral blood velocity (MCBv) and vice versa. This analysis is exploited to assess the efficiency of baroreflex and cerebral autoregulation. This study aims at characterizing CV and CBV controls in postural orthostatic tachycardiac syndrome (POTS) subjects experiencing exaggerated sympathetic response during orthostatic challenge via unconditional TE and TE conditioned on respiratory activity (R). *Approach.* In 18 healthy controls (age: 28 $\pm$ 13 yrs; 5 males, 13 females) and 15 POTS individuals (age: 29 $\pm$ 11 yrs; 3 males, 12 females) we acquired beat-to-beat variability of HP, SAP, MAP and MCBv and two R signals, namely respiratory chest movement (RCM) and capnogram (CAP). Recordings were made at sitting rest and during active standing (STAND). TE was computed via vector autoregressive approach. *Main results.* We found that: (i) when assessing CV interactions, the increase of the TE from SAP to HP during STAND, indicating baroreflex activation, is detected solely when conditioning on RCM; (ii) when assessing CBV interactions, the impact of R on the TE computation is negligible; (iii) POTS shows baroreflex impairment during STAND; (iv) POTS exhibits a normal CBV response to STAND. *Significance.* TE is useful for detecting the impairment of specific regulatory mechanisms in POTS. Moreover, using different R signals highlights the sensitivity of CV and CBV controls to specific R aspects.

1. Introduction

The cardiovascular (CV) and cerebrovascular (CBV) controls are essential for life. An impairment of the baroreflex reducing the amplitude of the changes of heart period (HP) per unit modification of systolic arterial pressure (SAP) (Pinna *et al* 2017) might lead to excessive variability of arterial pressure (AP) under orthostatic stimulus (Taylor and Eckberg 1996) and to postural intolerance (Farquhar *et al* 2000). Dysfunction of CBV control can lead to variable mean cerebral blood flow (MCBF) approximated as mean cerebral blood velocity (MCBv) under the hypothesis of invariance of the vessel diameter (Aaslid *et al* 1982), in response to physiological changes of mean arterial pressure (MAP) (Zhang *et al* 2002, Nakagawa *et al* 2011, Otite *et al* 2014), eventually

inducing hyperemia with a higher risk of stroke (Joshi *et al* 2010), ischemia with insufficient oxygen supply to the brain (Tarumi *et al* 2014) or hypoperfusion contributing to postural syncope (Carey *et al* 2001). Since CV and CBV regulations act in a closed loop, their impairment might not be merely related to the arm from SAP to HP (Porta *et al* 2000, Laude *et al* 2004) and from MAP to MCBv (Tiecks *et al* 1995, Panerai *et al* 1999a, Tzeng *et al* 2014, Gelpi *et al* 2022a) but also on the reverse pathways linked respectively to the balance between Frank-Starling law and diastolic runoff (Baselli *et al* 1994, Porta *et al* 2013a) and to the Cushing reflex elicited by hypoperfusion or intracranial pressure rise (Cushing 1902, Bari *et al* 2017, McBryde *et al* 2017, Saleem *et al* 2018, Bari *et al* 2021, Porta *et al* 2022).

Since CV and CBV variability interactions result from closed loop mechanisms, causality analysis accounting for the directionality of the influences seems to be a valid tool (Porta and Faes 2016). Among viable causality analysis tools, transfer entropy (TE), measuring the uncertainty decrement about the current state of the target when the behavior of the driver was considered above and beyond the past of the target and all conditioning factors recorded during the experimental session (Schreiber 2000, Barnett *et al* 2009, Vicente *et al* 2011), is particularly suitable for assessing CV and CBV control mechanisms (Faes *et al* 2013b, Porta *et al* 2015, Bari *et al* 2017, de Abreu *et al* 2020, Porta *et al* 2022). The TE is especially efficient in accounting for conditioning factors such as respiratory activity (*R*) when CV and CBV variability interactions are evaluated (Porta *et al* 2015, Porta *et al* 2022). On the CV side, R modulates vagal outflow directed to the sinus node (Porta *et al* 2000, Eckberg 2003) and solicited baroreceptors via modifications of intrathoracic pressure (De Boer *et al* 1987). On the CBV side, periodic movements of cerebrospinal fluid, induced by respiratory-related changes of intrathoracic pressure acting on thoracic and epidural veins lining the spine (Yildiz *et al* 2017, Porta *et al* 2022), directly disturb intracranial pressure, and, in turn, MCBv, while modifications of the venous return and stroke volume induce respiratory-related oscillations of MAP (Toska and Eriksen 1993, Caiani *et al* 2002, Elstad *et al* 2018).

When studying HP and SAP variability interactions, *R* is usually monitored via respiratory chest movement (RCM) (Faes *et al* 2013b, Porta *et al* 2015, Bari *et al* 2017, de Abreu *et al* 2020, Porta *et al* 2022). Conversely, capnogram (CAP) monitoring the inhaled and exhaled partial pressure of carbon dioxide (pCO_2) associated with *R* might be a more natural choice in setup designed to assess CBV control (Ogoh 2019). It is unclear whether different types of *R* monitoring might modify conclusions on CV and CBV variability interactions when TE conditioned on *R* is computed.

Thus, the study aims at evaluating the impact of different *R* signals (i.e. RCM and CAP) on directionality in CV and CBV variability interactions. TE from SAP to HP and vice versa and from MAP to MCBv and vice versa were computed. Unconditional TE was accompanied with TEs conditioned on *R* taken as RCM or CAP. The significance of the indexes was tested via surrogate data approach. The approach was tested on healthy subjects and patients with postural orthostatic tachycardia syndrome (POTS). The application in POTS is motivated by the fact that POTS patients are known to feature an exacerbated sympathetic activation during orthostatic challenge that affects baroreflex control (Farquhar *et al* 2000, Muenter Swift *et al* 2005, Barbic *et al* 2020), while little information is present about CBV regulation and limited to traditional parameters extracted from MCBv that do allow the assessment of the dynamic cerebral autoregulation (Wells *et al* 2020). Preliminary results were presented at the 12th meeting of the European Study Group on CV Oscillations (Gelpi *et al* 2022b).

2. Materials and methods

2.1. Experimental protocol

The data belonged to a database designed to assess the impact of sustained cognitive stress on CBV hemodynamics in POTS (Wells *et al* 2020). We referred to Wells *et al* (2020) for demographics and baseline physiological characteristics as well as types of medication. The protocol adhered to the principles of the Declaration of Helsinki for medical research involving human subjects. Subjects were enrolled at the Center for Heart Rhythm Disorders, The University of Adelaide, Australia. The experimental protocol was approved by the local institutional human research ethics committee. All participants provided written informed consent before their inclusion in the protocol. Briefly, we considered POTS patients ($n = 15$; age: 29 ± 11 yrs; 3 males, 12 females) and a cohort of age- and sex-matched healthy subjects (CONTROL $n = 18$; age: 28 ± 13 yrs; 5 males, 13 females). The enrolled POTS patients featured the typical symptoms of this syndrome (Wells *et al* 2020). The healthy status of CONTROL subjects was confirmed by clinical evaluation, checking their CV response to active standing and completing symptom questionnaires that indicated they did not have orthostatic intolerance.

All subjects underwent continuous monitoring of CV, CBV and *R* signals. More specifically, we acquired a single-lead electrocardiogram (ECG) via a commercial bioamplifier (FE132 Bioamp, ADInstruments Pty Ltd, NSW, Australia) and noninvasive AP using a cuff placed on the middle finger of the right hand via a volume-clamp device (Finapres Medical Systems BV, Enschede, The Netherlands). RCM was recorded via a

piezoresistive thoracic belt (MLT 1132/D Piezo Respiratory Belt Transducer, ADInstruments Pty Ltd, NSW, Australia). CAP (Capnostream 20P, Medtronic, Minneapolis, MN, USA) was acquired using nasal prongs with mouth scoop (Smart CapnoLine Plus, Microstream, Medtronic). Lastly, a transcranial Doppler device (Doppler-BoxX, Compumedics DWL, Singen, Germany) was used to monitor cerebral blood flow (CBF) via the measurement of cerebral blood velocity (CBv) from the middle cerebral artery in the dominant hemisphere. CBv was considered a proxy of CBF under the hypothesis of negligible modifications of the vessel diameter (Aaslid *et al* 1982). All signals were sampled simultaneously and continuously through a data acquisition device (Powerlab PL35/16, ADInstruments Pty Ltd, NSW, Australia) at a sampling rate of 1000 Hz.

Experiments took place in the morning in a temperature-controlled room, with patients abstaining from alcohol and caffeine over the preceding 24 h. Signals were recorded while sitting at rest (REST) and during active standing (STAND). STAND session followed the REST one. All participants with POTS were on treatment in accordance with current guidelines without any modification of the therapy in the previous month. Patients under vasopressors medications were asked to postpone the daily dose after completing the experiment.

2.2. Extraction of beat-to-beat variability series

From the ECG, the *R*-wave peaks were detected using a threshold on the first derivative. The *k*th HP, where *k* is the cardiac beat counter, was computed as the time distance between two consecutive *R*-wave peaks. The *k*th SAP and diastolic AP (DAP) were located at the timing of the maximum AP within the *k*th cardiac cycle and of the following minimum. The *k*th MAP was computed as the ratio of the definite integral of AP between the $(k-1)$th and *k*th DAP occurrences to the interdiastolic interval. The same procedure was applied to CBv to compute MCBv (Bari *et al* 2016). The CAP signal was filtered via a four-order low-pass Butterworth filter with a cutoff frequency of 0.5 Hz. The RCM and CAP signals were sampled in correspondence to the first *R*-wave peak delimiting the *k*th HP. The end-tidal pCO_2 ($etCO_2$), reflecting pCO_2 in the alveolar air, was taken as the sampling of CAP at the end of expiration, namely at the end of its relatively horizontal plateau phase, once per respiratory cycle. The resulting series were manually corrected in the case of missing beats or misdetections. The effect of ectopic beats, or isolated arrhythmic events, was mitigated via linear interpolation. Corrections did not exceed 5% of the total sequence length. Sequences of 250 consecutive beats were selected at REST and during STAND with the onset of the sequence randomly selected within the session. Representative examples of variability series are reported in figure 1 for a CONTROL subject at REST.

2.3. Computation of time and frequency domain variability markers

In the time domain, we computed the mean and variance of HP, SAP, MAP, and MCBv labeled, respectively, μ_{HP}, σ^2_{HP}, μ_{SAP}, σ^2_{SAP}, μ_{MAP}, σ^2_{MAP}, μ_{MCBv} and σ^2_{MCBv}. The indexes were expressed in ms, ms^2, mmHg, $mmHg^2$, mmHg, $mmHg^2$, cm s^{-1}, and cm^2 s^{-2}, respectively. The mean of $etCO_2$ was computed as well, denoted with μ_{etCO2} and expressed in mmHg.

In the frequency domain, parametric power spectral analysis was carried out according to an autoregressive (AR) representation of the series (Task Force 1996). The coefficients of the AR model and the variance of the white noise were estimated by solving the least squares problem via the Levinson–Durbin recursion (Baselli *et al* 1997). The number of coefficients was chosen from 4 to 16 according to the Akaike's figure of merit (Akaike 1974).

As to the CV analysis, we computed the power of HP in the high frequency (HF) band, from 0.15 to 0.40 Hz, and the power of SAP in the low frequency (LF) band, from 0.04 to 0.15 Hz, expressed in absolute units (i.e. ms^2 and $mmHg^2$), denoted respectively as HF_{HP} and LF_{SAP}. They were taken, respectively, as a marker of vagal modulation (Pomeranz *et al* 1985, Task Force 1996) and sympathetic modulation (Pagani *et al* 1997, Marchi *et al* 2016a).

As to the CBV analysis, the power of MAP and MCBv series was divided into the traditional bands optimized to describe the CBV regulation, namely very low frequency (VLF), from 0.02 to 0.07 Hz, LF from 0.07 to 0.15 Hz, and HF from 0.15 to 0.4 Hz (Claassen *et al* 2016). The superior cutoff of the LF power was limited to 0.15 Hz compared to suggestions given in Claassen *et al* (2016) because the respiratory rate might be slower than 0.2 Hz in CONTROL subjects (Vaini *et al* 2019). The powers of the MAP and MCBv series were expressed in absolute units (i.e. $mmHg^2$ and cm^2 s^{-2}) and labeled VLF_{MAP}, VLF_{MCBv}, LF_{MAP}, LF_{MCBv}, HF_{MAP} and HF_{MCBv}.

As to *R* signal, the frequency of the dominant oscillation of RCM and CAP series within the HF band from 0.15 to 0.4 Hz wasevaluated. They were indicated as f_{RCM} and f_{CAP}, respectively, and expressed in breaths per minute (bpm).

2.4. Estimation of TE and conditional TE

TE was computed according to the model-based approach reported in Barnett *et al* (2009), Porta *et al* (2015). Briefly, being *x*, *y* and *z*, the variability series describing the activity of the driver, the target and the conditioning

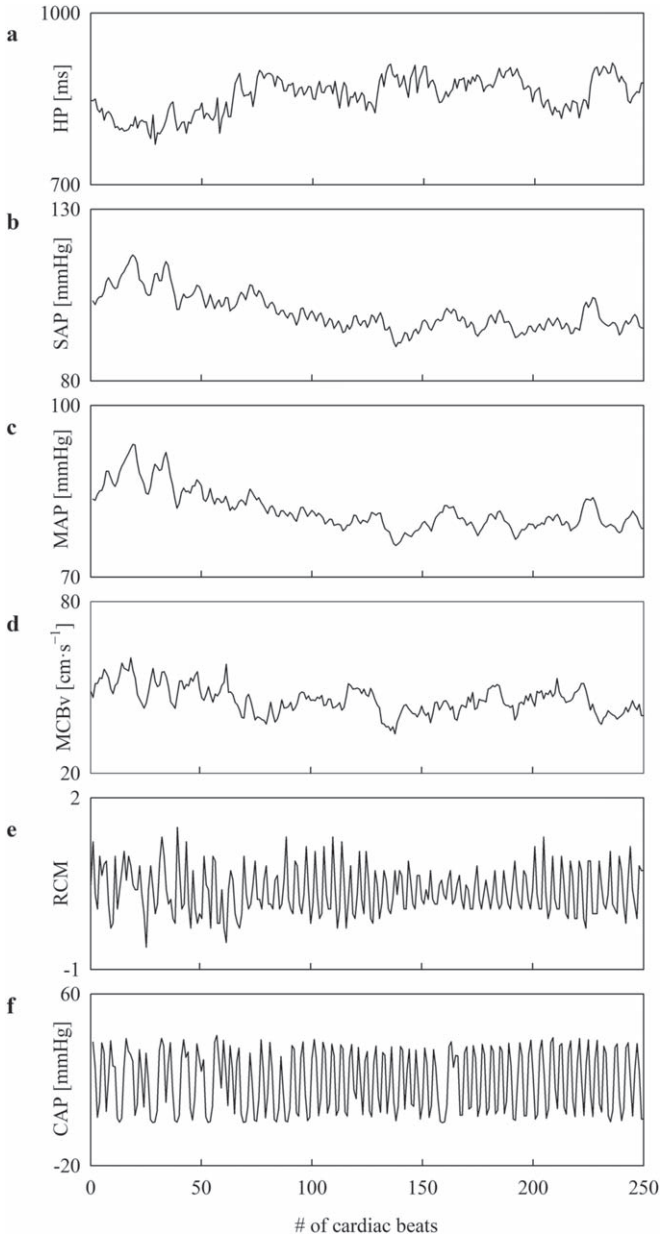

Figure 1. The line graphs show sequences of 250 consecutive values of HP (a), SAP (b), MAP (c), MCBv (d), RCM (e), and CAP (f) acquired from a CONTROL subject at REST.

system, we denoted the full Universe of knowledge with $\Omega = \{x, y, z\}$ and the restricted Universes of knowledge with $\Omega\backslash\{x\} = \{y, z\}$, $\Omega\backslash\{z\} = \{x, y\}$ and $\Omega\backslash\{x, z\} = \{y\}$ obtained from Ω by excluding, respectively, x, z, and both x and z. In Ω, $\Omega\backslash\{x\}$, $\Omega\backslash\{z\}$ and $\Omega\backslash\{x, z\}$ the current sample of y was explained as a linear combination of p past samples of all the signals present in the Universe of knowledge plus the current sample of a realization of a Gaussian white noise according to an AR model over y with double exogenous (XX) input (ARXX) over x and z in the case of Ω, to an AR model over y with single exogenous (X) input (ARX) over z in the case of $\Omega\backslash\{x\}$, to an ARX model over x in the case of $\Omega\backslash\{z\}$ and to an AR model over y in the case of $\Omega\backslash\{x, z\}$. After identifying the coefficients of the models, y was predicted by filtering the series with the identified coefficients and the prediction error variance was estimated as the average squared difference between the current and predicted sample computed over the entire series. Defined $\sigma^2_{y|yxz}$, $\sigma^2_{y|yz}$, $\sigma^2_{y|yx}$ and $\sigma^2_{y|y}$ the prediction error variances computed in Ω, $\Omega\backslash\{x\}$, $\Omega\backslash\{z\}$ and $\Omega\backslash\{x, z\}$ respectively, the conditional TE from x to y given z is given by

$$\mathrm{TE}_{x\to y|z} = 0.5 \cdot \log \frac{\sigma^2_{y|yz}}{\sigma^2_{y|yxz}}, \tag{1}$$

while the unconditional TE from x to y is given by

$$TE_{x\to y} = 0.5 \cdot \log \frac{\sigma^2_{y|y}}{\sigma^2_{y|yx}}. \quad (2)$$

Both $TE_{x\to y}$ and $TE_{x\to y|z}$ represent the information transfer from x to y but only $TE_{x\to y|z}$ accounts for the confounding influences of z (Barnett *et al* 2009, Porta *et al* 2015).

The coefficients of the ARXX, ARX, and AR models were estimated by solving traditional least squares problems via the Cholesky decomposition method (Baselli *et al* 1997). The number p of the coefficients weighting past samples was optimized in Ω for (1) and in $\Omega\backslash\{z\}$ for (2) via the Akaike criterion for multivariate processes (Akaike 1974) in the range from 6 to 14 and adopted, respectively, in $\Omega\backslash\{x\}$ and $\Omega\backslash\{x, z\}$ as well (Porta *et al* 2015). Since the coefficients of ARXX, ARX, and AR models were estimated via separate identification procedures, a double regression approach was exploited (Porta *et al* 2015). The latency of the actions of the driver and confounding factor on the target signal was set according to physiological considerations. The latency from SAP to HP was set to 0 beats and the latency from HP to SAP to 1 beat because the rapidity of the baroreflex allowed the kth SAP to prolong the kth HP, while the measurement conventions prevented the kth HP to modify the kth SAP and allowed it to act on the $(k + 1)$th SAP (Baselli *et al* 1994, Porta *et al* 2011). The latency from MAP to MCBv was set to 2 beats and the latency from MCBv to MAP to 0 beats, thus accounting for the capacitive and inertial properties of the pressure-to-flow pathway and fast responses of the flow-to-pressure link driven by the rapidity of barosensitive areas in the brain stem (Vaini *et al* 2019, Bari *et al* 2021). The latency from R signal to HP, SAP, MAP and MCBv was set to 0 beats (Porta *et al* 2015, Porta *et al* 2022). For the assessment of CV variability interactions, TE was computed in $\Omega = \{\text{SAP, HP, } R\}$, while for the assessment of CBV variability interactions, TE was computed in $\Omega = \{\text{MAP, MCBv, } R\}$. R was taken as a confounding factor and set to be either RCM or CAP. To derive information about closed loop CV and CBV variability interactions, we considered $x =$ SAP and $y =$ HP and vice versa and $x =$ MAP and $y =$ MCBv and vice versa. Therefore, we computed the following conditional TEs: $TE_{SAP\to HP|RCM}$, $TE_{SAP\to HP|CAP}$, $TE_{HP\to SAP|RCM}$, $TE_{HP\to SAP|CAP}$, $TE_{MAP\to MCBv|RCM}$, $TE_{MAP\to MCBv|CAP}$, $TE_{MCBv\to MAP|RCM}$, and $TE_{MCBv\to MAP|CAP}$, as well as the following TEs: $TE_{SAP\to HP}$, $TE_{HP\to SAP}$, $TE_{MAP\to MCBv}$, and $TE_{MCBv\to MAP}$. All variability series were normalized by subtracting their mean and by dividing the result by the standard deviation. TE and conditional TE were computed in each subject in any experimental condition and values were pooled together as well to compare results derived from different modalities of the TE computation. Variation of TE from STAND to REST (ΔTE) was assessed over the same individual.

2.5. Testing the null hypothesis of uncoupling between two series

We tested the null hypothesis of absence of dynamic interactions among series (H_0) by assessing unconditional TE and conditional TE over surrogate series built from their original versions with the aim at destroying all possible links, while preserving amplitude distribution and power spectral density (Porta and Faes 2016). Surrogate data set were built individually over each subject in any experimental condition using the technique of time shifting the original version of the series, thus destroying the cross-correlation, while preserving autocorrelation and amplitude distribution (Andrzejak *et al* 2003, Porta *et al* 2015). As to the CV analysis, HP series was left unmodified, while SAP, RCM and CAP sequences were shifted. As to the CBV analysis, MCBv series was left unmodified, while MAP, RCM and CAP were shifted. The delay was chosen randomly between 40 and 80 cardiac beats. The values at the end of the shifted series were wrapped to its onset. For each original set of series, we built 100 surrogate pairs. Unconditional TE and conditional TE were computed over the original and surrogates. The marker calculated over the original sequences was deemed to be significantly greater than 0 whether it was above the 95th percentile of the distribution of the marker assessed over the set of surrogates. In this case we rejected H_0. The percentage of subjects in which H_0 was rejected was computed for unconditional TE and conditional TE for each population and experimental condition. These markers were labeled $TE_{SAP\to HP}$%, $TE_{HP\to SAP}$%, $TE_{MAP\to MCBv}$%, $TE_{MCBv\to MAP}$% and $TE_{SAP\to HP|RCM}$%, $TE_{SAP\to HP|CAP}$%, $TE_{HP\to SAP|RCM}$%, $TE_{HP\to SAP|CAP}$%, $TE_{MAP\to MCBv|RCM}$%, $TE_{MAP\to MCBv|CAP}$%, $TE_{MCBv\to MAP|RCM}$%, $TE_{MCBv\to MAP|CAP}$%. To compare results derived from different modalities of computation of TE the outcomes of the surrogate test were pooled together regardless of the group and experimental condition as well.

2.6. Statistical analysis

Normality was tested via the Shapiro–Wilk test. Two-way repeated measures analysis of variance (one factor repetition, Holm-Sidak test for multiple comparisons) was applied to time, frequency, and information domain markers to assess the effect of the experimental condition (i.e. REST or STAND) within the same group (i.e. CONTROL and POTS) and the significance of the between-group differences within the same experimental condition. Two-way repeated measures analysis of variance (one factor repetition, Holm-Sidak test for multiple

Table 1. Time and frequency domain CV indexes in CONTROL and POTS groups at REST and during STAND.

CV index	CONTROL		POTS	
	REST	STAND	REST	STAND
μ_{HP} (ms)	814.3 ± 113.8	735.9 ± 118.8*	723.6 ± 139.1§	654.3 ± 149.3*
σ^2_{HP} (ms^2)	3358.3 ± 2717.7	2206.3 ± 1674.2	1473.8 ± 1147.6	1623.2 ± 1695
HF_{HP} (ms^2)	904.4 ± 1048	506.8 ± 714.6	348.8 ± 311.9	369.4 ± 635.5
μ_{SAP} (mmHg)	108.2 ± 19.2	117.8 ± 23.4*	118.2 ± 14	129.9 ± 15.6*§
σ^2_{SAP} (mmHg^2)	14.8 ± 8	19 ± 11.6	14.6 ± 13.3	19.4 ± 13.8
LF_{SAP} (mmHg^2)	3.4 ± 4.5	5.3 ± 7.3	2.2 ± 2.7	10.7 ± 9.6*§

CV = cardiovascular; μ = mean; σ^2 = variance; HP = heart period; SAP = systolic arterial pressure; LF = low frequency; HF = high frequency; CONTROL = healthy age-matched population; POTS = postural orthostatic tachycardia syndrome; REST = while sitting at rest; STAND = during active standing. The symbol * indicates a significant difference versus REST within the same group (i.e. CONTROL or POTS) with $p < 0.05$. The symbol § indicates a significant difference versus CONTROL within the same experimental condition (i.e. REST or STAND) with $p < 0.05$.

comparisons) was applied to ΔTE to assess the impact of the conditioning signal (i.e. RCM or CAP) within the same group and the significance of the between-group differences using the same conditioning signal. One-way repeated measures analysis of variance (Tukey test for multiple comparisons), or one-way Friedman repeated measures analysis of variance on ranks (Tukey test for multiple comparisons), when appropriate, was used to compare unconditional TE and conditional TE after pooling together data regardless of the group and experimental condition. The dependence of the significance of the dynamical interactions on the experimental condition and group was assessed via $\chi 2$ test applied to the proportion of subjects featuring the rejection of the uncoupling hypothesis. The comparison between REST and STAND accounted for the application of the test over the same subject via McNemar's test. The level of significance of the test was lowered according to the number of comparisons (i.e. 4) to account for the multiple comparison issue. The same test was applied to compare the percentages of rejection of uncoupling hypothesis derived from the TE types after pooling together all the outcomes of the surrogate test regardless of the group and experimental condition. In this case the level of significance of the test was lowered 3 times to account for the multiple comparison issue. Data are expressed as mean ± standard deviation. Statistical analysis was carried out using a commercial statistical program (Sigmaplot, v.14.0, Systat Software, Inc., Chicago, IL, United States). A type I error probability $p < 0.05$ was always considered statistically significant.

3. Results

3.1. Results of time and frequency domain variability analysis

Table 1 summarizes CV indexes derived from HP and SAP variability series. Orthostatic stimulus caused the shortening of μ_{HP} in both populations (i.e. CONTROL and POTS). Moreover, POTS were more tachycardic at REST than CONTROL subjects. μ_{SAP} increased during STAND in both groups being the values of μ_{SAP} during STAND in POTS greater than in CONTROL individuals. The activation of the sympathetic control during STAND was also suggested by the increase of the LF_{SAP} power but its increment was visible solely in POTS and much more relevant than that in CONTROL group. σ^2_{HP}, HF_{HP}, and σ^2_{SAP} did not vary across groups and experimental conditions.

Table 2 outlines CBV indexes derived from MAP and MCBv variability series. Postural challenge induced the increase of μ_{MAP}, and the rise was more important in POTS group. σ^2_{MAP} increased significantly with STAND solely in POTS and the rise of the MAP variability occurred in the LF band. During STAND, the HF_{MAP} power was larger in POTS than in CONTROL individuals. STAND induced the decrease of μ_{MCBv} in both populations. The HF_{MCBv} power increased during STAND compared to REST solely in POTS patients, and during STAND, it was larger in POTS individuals compared to CONTROL subjects. VLF_{MAP}, σ^2_{MCBv}, VLF_{MCBv}, and LF_{MCBv} did not vary across groups and experimental conditions.

Table 3 summarizes respiratory indexes derived from RCM and CAP. The respiratory frequency (i.e. f_{RCM} and f_{CAP}) remained stable across experimental conditions and populations regardless of the respiratory signal. μ_{etCO2} did not vary with either experimental condition or group as well.

3.2. Results of unconditional TE and TE conditioned on *R* signal

The vertical simple error bar graphs of figure 2 compare the information transfer computed from SAP to HP (figure 2(a)), from HP to SAP (figure 2(b)), from MAP to MCBv (figure 2(c)) and from MCBv to MAP (figure 2(d)) derived via unconditional TE, TE conditioned on RCM and TE conditioned on CAP. Data were

Table 2. Time and frequency domain CBV indexes in CONTROL and POTS groups at REST and during STAND.

CBV index	CONTROL		POTS	
	REST	STAND	REST	STAND
μ_{MAP} (mmHg)	82.2 ± 16.8	92 ± 20*	91.1 ± 12.3	102.8 ± 15.2*§
σ^2_{MAP} (mmHg^2)	6.2 ± 3.7	7.5 ± 4.3	5.9 ± 2	9 ± 5.3*
VLF_{MAP} (mmHg^2)	1.6 ± 3.1	2 ± 2.9	1.8 ± 2.7	1.1 ± 3.2
LF_{MAP} (mmHg^2)	1.3 ± 1.8	3.5 ± 5.1	1.7 ± 1.9	5.3 ± 5.2*
HF_{MAP} (mmHg^2)	0.3 ± 0.3	0.3 ± 0.4	0.6 ± 0.5	0.7 ± 0.5§
μ_{MCBv} (cm s^{-1})	55.2 ± 14.9	52.7 ± 13.7*	55.2 ± 15.6	53.3 ± 17.1*
σ^2_{MCBv} (cm^2 s^{-2})	28.5 ± 19.5	40.3 ± 30.2	30.1 ± 17.9	45.6 ± 26.8
VLF_{MCBv} (cm^2 s^{-2})	6.2 ± 15.3	14.2 ± 27.3	4.5 ± 9.2	10.9 ± 22.8
LF_{MCBv} (cm^2 s^{-2})	6.9 ± 9.7	8.2 ± 11.3	5.3 ± 9.6	7.9 ± 8.3
HF_{MCBv} (cm^2 s^{-2})	2 ± 1.7	3.3 ± 3.8	3 ± 2.2	5.6 ± 5.3*§

CBV = cerebrovascular; μ = mean; σ^2 = variance; MCBv = mean cerebral blood velocity; MAP = mean arterial pressure; LF = low frequency; VLF = very LF; HF = high frequency; CONTROL = healthy age-matched population; POTS = postural orthostatic tachycardia syndrome; REST = while sitting at rest; STAND = during active standing. The symbol * indicates a significant difference versus REST within the same group (i.e. CONTROL or POTS) with $p < 0.05$. The symbol § indicates a significant difference versus CONTROL within the same experimental condition (i.e. REST or STAND) with $p < 0.05$.

Table 3. *R* activity indexes in CONTROL and POTS groups at REST and during STAND.

R index	CONTROL		POTS	
	REST	STAND	REST	STAND
f_{RCM} (bpm)	17.7 ± 4.5	17.1 ± 3.9	16.7 ± 3.8	17.7 ± 2.8
f_{CAP} (bpm)	17.2 ± 3.5	16 ± 3.3	16 ± 2.7	16.7 ± 3.5
μ_{etCO2} (mmHg)	39 ± 3.5	38.3 ± 4.3	38.7 ± 3.1	37.5 ± 2.9

R = respiratory activity; RCM = respiratory chest movement; CAP = capnogram; pCO_2 = partial pressure of the carbon dioxide; $etCO_2$ = end-tidal pCO_2; μ_{etCO2} = mean of $etCO_2$; bpm = breaths per minute; CONTROL = healthy age-matched population; POTS = postural orthostatic tachycardia syndrome; REST = while sitting at rest; STAND = during active standing.

pooled together regardless of the experimental condition (i.e. REST or STAND) and group (i.e. CONTROL or POTS). TE from SAP to HP conditioned on RCM was smaller than unconditional TE from SAP to SAP and TE from SAP to HP conditioned on CAP. No difference between different modalities for the computation of TE was detected from HP and SAP, from MAP to MCBv and from MCBv to MAP.

The vertical simple bar graphs of figure 3 compare the percentage of rejections of H_0 from SAP to HP (figure 3(a)), from HP to SAP (figure 3(b)), from MAP to MCBv (figure 3(c)) and from MCBv to MAP (figure 3(d)) as a function of the modality of the TE computation (i.e. unconditional TE, TE conditioned on RCM and TE conditioned on CAP). Data were pooled together regardless of the experimental condition (i.e. REST or STAND) and group (i.e. CONTROL or POTS). When assessing both CV and CBV dynamic interactions no difference between different modalities for the TE computation was detected.

Table 4 summarizes the unconditional TE computed over CV and CBV variability series in CONTROL and POTS subjects at REST and during STAND. As to CV variability interactions, TE from HP to SAP decreased during STAND in both CONTROL and POTS groups, while TE from SAP to HP remained stable across experimental conditions in both groups. TE from SAP to HP and TE from HP to SAP did not vary across groups, and this result held regardless of the experimental condition. As to CBV variability interactions, TE from MAP to MCBv and TE from MCBv to MAP were not affected by either experimental condition or group.

Table 5 lists the percentage of subjects featuring the rejection of the uncoupling hypothesis using unconditional TE computed over CV and CBV variability series in CONTROL and POTS subjects at REST and during STAND. Regardless of the type of dynamic interactions (i.e. CV or CBV) the percentage was high in any experimental condition and group. The smallest percentages were 78% and 63% over CV and CBV variability series, respectively. Differences between groups within the same experimental condition and between experimental conditions within the same group were not detected.

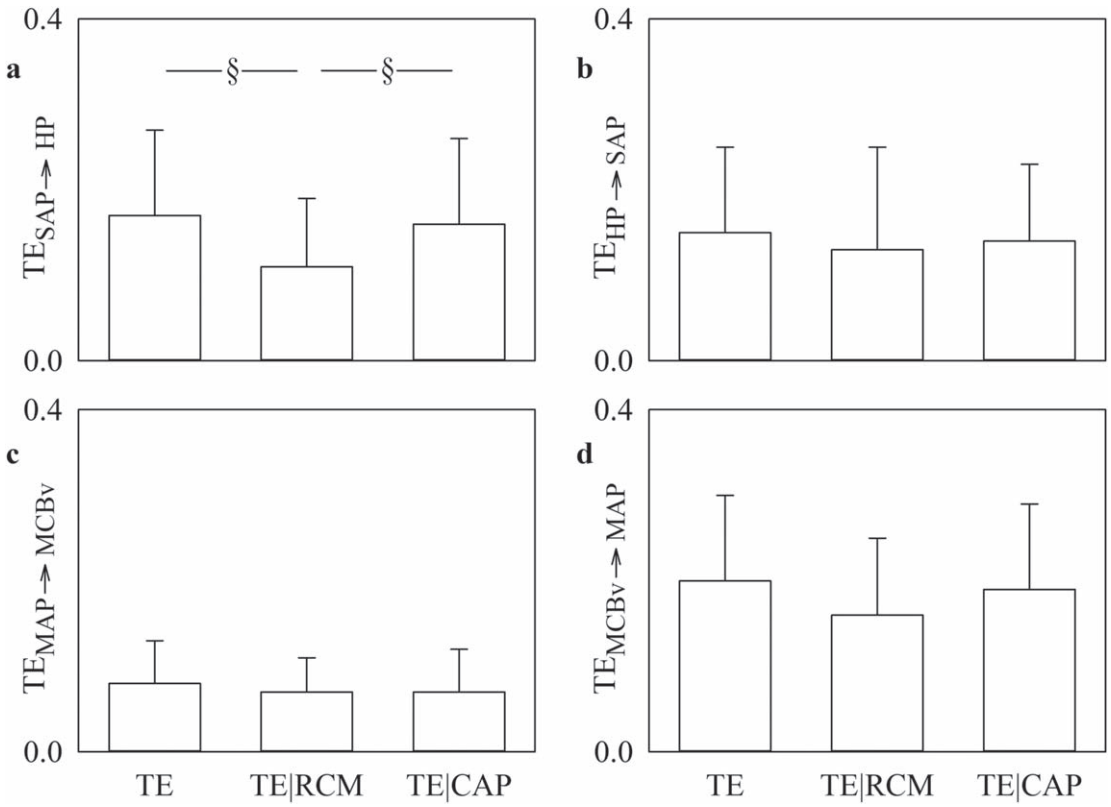

Figure 2. The vertical simple error bar graphs show the TE from SAP to HP (a), from HP to SAP (b), from MAP to MCBv (c) and from MCBv to MAP (d) as a function of modality of its computation (i.e. unconditional TE, TE conditioned on RCM and TE conditioned on CAP). Data are pooled together regardless of the experimental condition (i.e. REST or STAND) and group (i.e. CONTROL or POTS). The symbol § between modality of TE computation with $p < 0.05$.

Table 6 summarizes the values of TE conditioned on *R* signals, namely RCM and CAP, computed over CV and CBV variability series in CONTROL and POTS subjects at REST and during STAND. As to CV variability interactions, TE from SAP to HP conditioned on RCM increased with STAND exclusively in the CONTROL group, while TE from SAP to HP conditioned on CAP did not vary during postural challenge. TE from HP to SAP conditioned on *R* decreased during STAND in the CONTROL group regardless of the type of conditioning signal (i.e. RCM or CAP). This decrement was visible only with CAP in POTS individuals. TE from SAP to HP and TE from HP to SAP did not separate CONTROL and POTS individuals, and this result held regardless of the experimental condition and type of conditioning signals. As to CBV variability interactions, STAND did not induce any change within the same group and POTS subjects could not be differentiated from CONTROL individuals within the same experimental condition. This result held regardless of the direction of the interactions, namely from MAP to MCBv and from MCBv to MAP, and type of conditioning signal.

Table 7 lists the percentage of subjects featuring the rejection of the uncoupling hypothesis using TE conditioned on *R* signals, namely RCM and CAP, computed over CV and CBV variability series in CONTROL and POTS subjects at REST and during STAND. The percentages were high in any experimental condition and group and this result held for both dynamic CV and CBV interactions. The smallest percentages were 67% and 61% over CV and CBV variability series, respectively. Percentages did not vary across groups and experimental conditions.

The grouped error bar graphs of figure 4 show ΔTE, namely the variation of TE induced by STAND as a function of the type of *R* signal (i.e. RCM and CAP) in CONTROL (black bars) and POTS (white bars) groups. Results of CV variability interactions are reported in figures 4(a), (b), while those of CBV directionality indexes are shown in figures 4(c), (d). ΔTE from SAP to HP was significantly higher when the conditioning signal was RCM than using CAP, while no difference was detected across groups (figure 4(a)). ΔTE from HP to SAP was similar across conditioning signals and groups (figure 4(b)). Both ΔTE from MAP to MCBv (figure 4(c)) and from MCBv to MAP (figure 4(d)) did not vary with either conditioning signal or group.

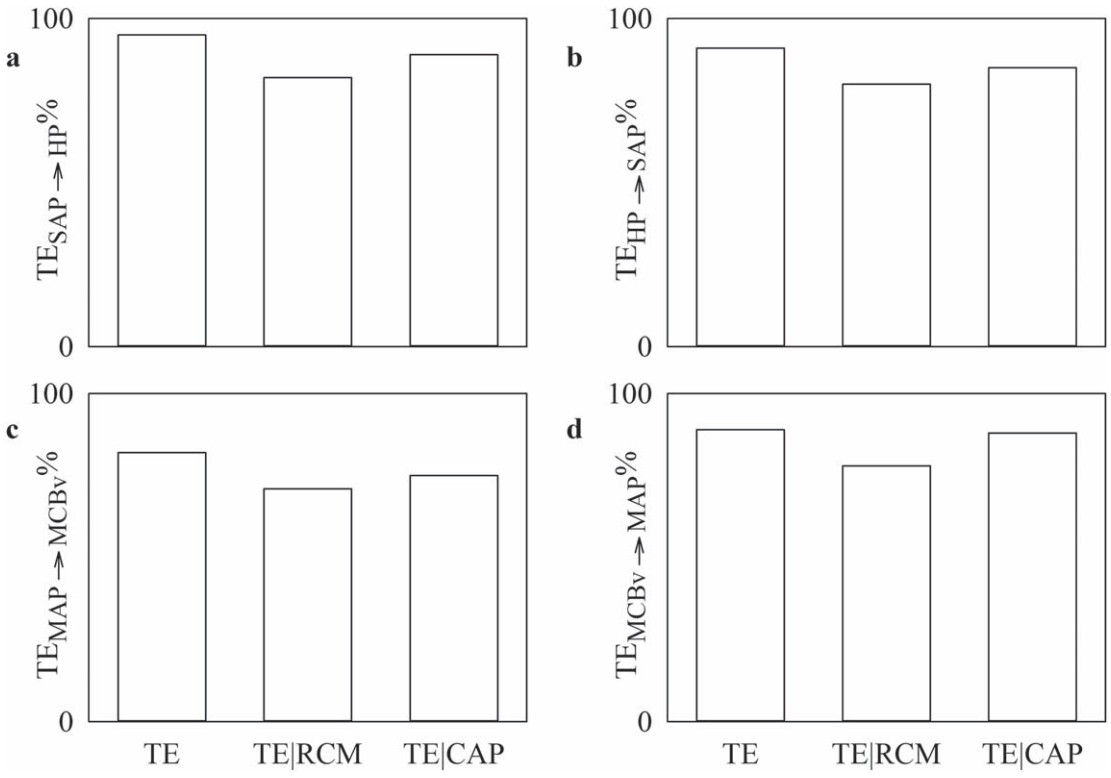

Figure 3. The vertical simple bar graphs show the percentage of H_0 rejections from SAP to HP (a), from HP to SAP (b), from MAP to MCBv (c) and from MCBv to MAP (d) as a function of modality of computation of the TE marker (i.e. unconditional TE, TE conditioned on RCM and TE conditioned on CAP). Data are pooled together regardless of the experimental condition (i.e. REST or STAND) and group (i.e. CONTROL or POTS).

Table 4. Uncondtional TE in CONTROL and POTS groups at REST and during STAND.

CV and CBV indexes	CONTROL		POTS	
	REST	STAND	REST	STAND
$TE_{SAP \rightarrow HP}$	0.16 ± 0.11	0.18 ± 0.2	0.17 ± 0.09	0.15 ± 0.08
$TE_{HP \rightarrow SAP}$	0.20 ± 0.14	$0.12 \pm 0.05^{*}$	0.16 ± 0.09	$0.09 \pm 0.05^{*}$
$TE_{MAP \rightarrow MCBv}$	0.06 ± 0.05	0.10 ± 0.05	0.08 ± 0.04	0.09 ± 0.04
$TE_{MCBv \rightarrow MAP}$	0.18 ± 0.10	0.16 ± 0.07	0.23 ± 0.1	0.23 ± 0.14

CV = cardiovascular; CBV = cerebrovascular; TE = transfer entropy; HP = heart period; SAP = systolic arterial pressure; MCBv = mean cerebral blood velocity; MAP = mean arterial pressure; CONTROL = healthy age-matched population; POTS = postural orthostatic tachycardia syndrome; REST = while seating at rest; STAND = during active standing. The symbol * indicates a significant difference versus REST within the same group (i.e. CONTROL or POTS) with $p < 0.05$.

4. Discussion

The main findings of the study can be summarized as follows: (i) surrogate data approach confirms the significance of CV and CBV dynamic interactions regardless of whether the influence of R is explicitly accounted for; (ii) when assessing CV variability interactions, the increase of the TE from SAP to HP during STAND is detected when conditioning out RCM, while it is not observed using unconditional TE and when TE is conditioned on CAP; (iii) when assessing CBV variability interactions, conclusions do not depend on the modality of the TE computation; (iv) POTS shows an abnormal CV response to STAND due to cardiac baroreflex impairment; (v) POTS shows a normal CBV response to STAND.

4.1. On the computation of TE to assess closed loop CV and CBV variability interactions

TE assesses the decrement of uncertainty occurring when the restricted Universe of knowledge is completed with the presumed cause. The TE conditioned on z is computed as the difference between the conditional entropies of y in

Table 5. Uncondtional TE-based percentage of rejections of the H_0 in CONTROL and POTS groups at REST and during STAND.

CV and CBV indexes	CONTROL		POTS	
	REST	STAND	REST	STAND
$TE_{SAP\rightarrow HP}$%	95	94	100	92
$TE_{HP\rightarrow SAP}$%	95	78	100	92
$TE_{MAP\rightarrow MCBv}$%	63	89	88	92
$TE_{MCBF\rightarrow MAP}$%	90	83	100	85

CV = cardiovascular; CBV = cerebrovascular; TE = transfer entropy; TE% = percentage of rejections of H_0; obtained via the test over TE; HP = heart period; SAP = systolic arterial pressure; MCBv = mean cerebral blood velocity; MAP = mean arterial pressure; CONTROL = healthy age-matched population; POTS = postural orthostatic tachycardia syndrome; REST = while seating at rest; STAND = during active standing.

Table 6. TE conditioned on *R* signal in CONTROL and POTS groups at REST and during STAND.

CV and CBV indexes	CONTROL		POTS	
	REST	STAND	REST	STAND
$TE_{SAP\rightarrow HP\|RCM}$	0.09 ± 0.05	$0.15 \pm 0.1^*$	0.09 ± 0.07	0.12 ± 0.06
$TE_{SAP\rightarrow HP\|CAP}$	0.13 ± 0.07	0.17 ± 0.14	0.18 ± 0.1	0.16 ± 0.07
$TE_{HP\rightarrow SAP\|RCM}$	0.16 ± 0.13	$0.11 \pm 0.06^*$	0.14 ± 0.06	0.08 ± 0.03
$TE_{HP\rightarrow SAP\|CAP}$	0.19 ± 0.13	$0.11 \pm 0.07^*$	0.16 ± 0.08	$0.09 \pm 0.05^*$
$TE_{MAP\rightarrow MCBv\|RCM}$	0.05 ± 0.04	0.08 ± 0.05	0.07 ± 0.04	0.07 ± 0.03
$TE_{MAP\rightarrow MCBv\|CAP}$	0.06 ± 0.07	0.08 ± 0.03	0.08 ± 0.04	0.08 ± 0.04
$TE_{MCBv\rightarrow MAP\|RCM}$	0.15 ± 0.08	0.2 ± 0.18	0.17 ± 0.1	0.16 ± 0.11
$TE_{MCBv\rightarrow MAP\|CAP}$	0.18 ± 0.1	0.16 ± 0.08	0.23 ± 0.09	0.22 ± 0.14

CV = cardiovascular; CBV = cerebrovascular; TE = transfer entropy; HP = heart period; SAP = systolic arterial pressure; MCBv = mean cerebral blood velocity; MAP = mean arterial pressure; *R* = respiratory activity; RCM = respiratory chest movement; CAP = capnogram; CONTROL = healthy age-matched population; POTS = postural orthostatic tachycardia syndrome; REST = while sitting at rest; STAND = during active standing. The symbol * indicates a significant difference versus REST within the same group (i.e. CONTROL or POTS) with $p < 0.05$.

Table 7. Conditional TE-based percentage of rejections of H_0 in CONTROL and POTS groups at REST and during STAND.

CV and CBV indexes	CONTROL		POTS	
	REST	STAND	REST	STAND
$TE_{SAP\rightarrow HP\|RCM}$%	74	89	87	77
$TE_{SAP\rightarrow HP\|CAP}$%	84	83	100	92
$TE_{HP\rightarrow SAP\|RCM}$%	84	67	93	77
$TE_{HP\rightarrow SAP\|CAP}$%	90	67	100	85
$TE_{MAP\rightarrow MCBv\|RCM}$%	61	67	80	85
$TE_{MAP\rightarrow MCBv\|CAP}$%	68	67	87	85
$TE_{MCBv\rightarrow MAP\|RCM}$%	84	67	87	77
$TE_{MCBv\rightarrow MAP\|CAP}$%	95	78	100	77

CV = cardiovascular; CBV = cerebrovascular; TE = transfer entropy; TE% = percentage of rejections of H_0; obtained via the test over TE; HP = heart period; SAP = systolic arterial pressure; MCBv = mean cerebral blood velocity; MAP = mean arterial pressure; *R* = respiratory activity; RCM = respiratory chest movement; CAP = capnogram; CONTROL = healthy age-matched population; POTS = postural orthostatic tachycardia syndrome; REST = while seating at rest; STAND = during active standing.

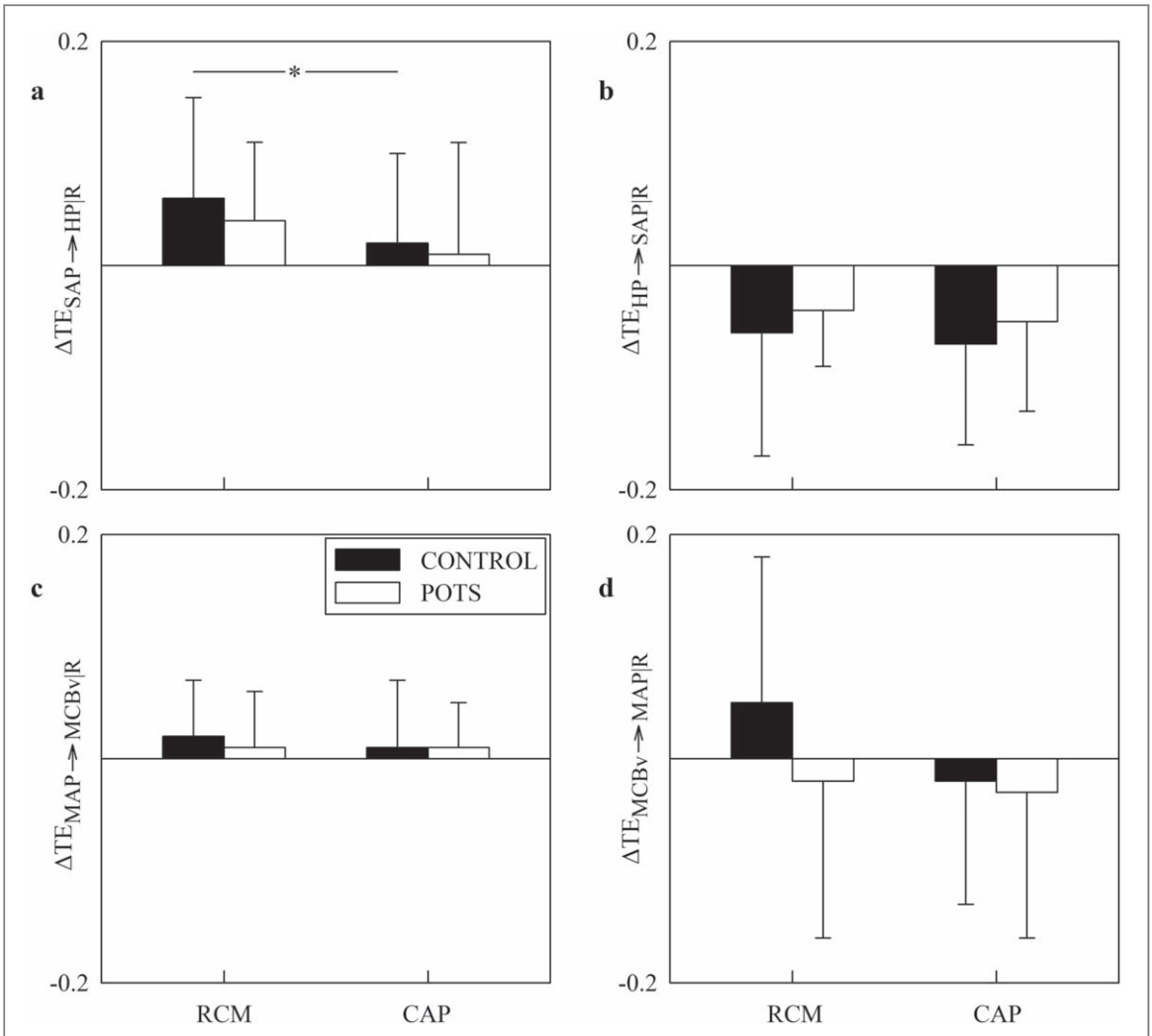

Figure 4. The vertical grouped error bar graphs show the TE variation from STAND to REST (ΔTE) as a function of the *R* signal, namely RCM and CAP, computed in CONTROL (black bars) and POTS (white bars) subjects. The TE markers are computed on the CV system in (a) and (b): from SAP to HP conditioned on *R* in (a) and from HP to SAP conditioned on *R* in (b). The TE markers are computed on the CBV system in (c) and (d): from MAP to MCBv conditioned on *R* in (c) and from MCBv to MAP conditioned on *R* in (d). The symbol * indicates a significant difference between R signals within the same group (i.e. CONTROL or POTS) with $p < 0.05$.

$\Omega\backslash\{x\}$ and Ω, while unconditional TE is computed as the difference between the conditional entropies of y in $\Omega\backslash\{x, z\}$ and $\Omega\backslash\{z\}$, where the conditional entropy quantifies the amount of information carried by y that cannot be derived from past values of all signals in $\Omega\backslash\{x\}$, Ω, $\Omega\backslash\{x, z\}$, and $\Omega\backslash\{z\}$. Vector AR model-based approach (Barnett *et al* 2009) allows the computation of the conditional entropies of y in $\Omega\backslash\{x\}$ and Ω from the variance $\sigma^2_{y|yz}$ of the innovation of the ARX model in $\Omega\backslash\{x\}$ as $0.5 \cdot \log(2\pi \cdot e \cdot \sigma^2_{y|yz})$ and from the variance $\sigma^2_{y|yxz}$ of the innovation of the ARXX model in Ω as $0.5 \cdot \log(2\pi \cdot e \cdot \sigma^2_{y|yxz})$, while the conditional entropies in $\Omega\backslash\{x, z\}$ and $\Omega\backslash\{z\}$ can be computed from the variance $\sigma^2_{y|y}$ of the innovation of the AR model in $\Omega\backslash\{x, z\}$ as $0.5 \cdot \log(2\pi \cdot e \cdot \sigma^2_{y|y})$ and from the variance $\sigma^2_{y|yx}$ of the innovation of the ARX model in $\Omega\backslash\{z\}$ as $0.5 \cdot \log(2\pi \cdot e \cdot \sigma^2_{y|yx})$, where e is the Nepero's number, thus justifying the compact formulas given in (1) and (2) (Porta *et al* 2017). TE holds the following properties: (i) it is in agreement with Granger causality definition because it is based on the comparison of the representation of y in a full and restricted Universes of knowledge (Granger 1980); (ii) it is independent of the absolute values of series as any information-theoretic metric (Schreiber 2000, Barnett *et al* 2009, Vicente *et al* 2011, Porta and Faes 2016); (iii) it is an asymmetric information-theoretic metric because reversing the role of x and y did not produce the same value (Schreiber 2000, Barnett *et al* 2009, Vicente *et al* 2011, Porta and Faes 2016); (iv) the significance of TE should be tested according to some null hypothesis (e.g. absence of dynamic interactions among signals as in this study) using an appropriate statistics or a surrogate data approach (Porta and Faes 2016).

4.2. Direct comparison of TE metrics

Unconditional TE and conditional TEs were explicitly compared after pooling together groups and experimental conditions.

This comparison in the time direction from SAP to HP indicates that the TE from SAP to HP decreased after conditioning out RCM compared to the unconditional TE and TE conditioned on CAP, thus suggesting that a part of the information transfer from SAP to HP was not the consequence of respiratory changes of SAP but it was driven directly by *R* influences better described by RCM. The direct effect of *R* was not evident in the causal direction from HP to SAP likely because the respiratory components of SAP were driven by respiratory sinus arrhythmia through the mechanical feedforward pathway. No evident difference was observed between the TEs from SAP to HP and the TEs from HP to SAP, thus indicating no prevalent direction of the information transfer in the CV closed loop. The similar, and high (above 80%), percentages of rejections of the HP-SAP uncoupling hypothesis across different TEs observed after pooling together groups and experimental conditions stress the importance of both causal relationships and closed loop CV interactions (Faes *et al* 2013a, Porta *et al* 2013b, Corbier *et al* 2020, Shankhwar *et al* 2022).

The comparison across TEs from MAP to MCBv and *vice versa* performed after pooling together groups and experimental conditions outlines that accounting for *R* when assessing CBV variability interactions did not change the information transfer and this conclusion held regardless of the directionality of interaction likely because variability at the respiratory rate in MAP and MCBv was not the genuine consequence of *R* but it was a rhythm transferred from MAP to MCBv and *vice versa*. The comparison between the TEs from MAP to MCBv and the TEs from MCBv to MAP suggests a prevalent information transfer along the flow-to-pressure pathway and remarks the importance of studying this pathway, especially in experimental conditions inducing a sympathetic activation and in populations featuring a high sympathetic drive. However, this finding might depend on the setting of the latencies in the modeling structure and this issue might deserve future investigations. We remark that the latencies set in the preset study have been optimized in the beat-to-beat domain over spontaneous variations and separately over the two pathways via a causality analysis (Vaini *et al* 2019, Bari *et al* 2021). Future analysis of the impact of the latencies on results provided by vector AR model should be performed by assessing different combinations of latencies in experimental situations featuring various autonomic nervous system states. The percentages of rejections of the MCBv-MAP uncoupling hypothesis across different TEs after pooling together groups and experimental conditions were similar and high (above 71%), even when the absolute values of TE were small (i.e. from MAP to MCBv). This result indicates the consistency of these interactions even in presence of mechanisms such as cerebral autoregulation that should contribute to their weak visibility (Saleem *et al* 2018, Vaini *et al* 2019, Porta *et al* 2022).

4.3. Closed loop CV variability interactions depend on the *R* signal

The information transfer along baroreflex, namely from SAP to HP, and along mechanical feedforward pathway, namely in the reverse causal direction from HP to SAP, was computed by disregarding and accounting *R* as a conditioning factor. Two different *R* signals representing different aspects of the physiology of the respiratory system (i.e. RCM and CAP) were considered. Results allowed us to assess the impact of *R* and the type of *R* signal on the evaluation of closed loop CV variability interactions. Tests on surrogate data indicated that significant CV dynamic interactions in any group in any experimental condition are detectable and this result holds regardless of the strategy adopted to account for *R* (i.e. TE types).

Without conditioning for *R* the increase of the TE from SAP to HP during STAND (Porta *et al* 2011, Faes *et al* 2013a, Porta *et al* 2015, Bari *et al* 2017), taken as a sign of baroreflex activation in response to the blood pooling in the lower extremities, was not detected. This result agrees with Porta *et al* (2012) that indicated the *R*, monitored via RCM, is a latent confounder of the baroreflex control because a portion of the HP variability directly driven by *R* is erroneously attributed to the action of SAP changes using an approach that does not include *R* as an additional exogenous signal. Remarkably, the major effect of disregarding the conditioning influence of *R* was visible at REST when vagal control is higher (Pomeranz *et al* 1985, Porta *et al* 2012) and took the form of a high value of the unconditional TE from SAP to HP. The impact of *R* on the reverse pathway (i.e. from HP to SAP) was less important and this result is supported by the observation that values of unconditional TE and conditional TE were similar.

In the present study we originally observe that conclusions about CV causality analysis depend on the type of the *R* signal. Indeed, the expected increase of the TE from SAP to HP during an orthostatic challenge, usually observed in healthy subjects (Porta *et al* 2011, Faes *et al* 2013a, Porta *et al* 2015, Bari *et al* 2017), could be detected only when RCM was utilized as a conditioning signal. This result is the likely consequence of the better reliability of RCM in representing a soliciting input driving respiratory sinus arrhythmia regardless of SAP changes compared to CAP. Conversely, RCM and CAP signals had a similar impact on conditional TE assessed from HP to SAP along the feedforward mechanical pathway likely because the genuine impact of *R* in driving SAP is limited compared to contributions modulating ventricular filling and diastolic runoff (Baselli *et al* 1994, Porta *et al* 2013a).

4.4. Closed loop CBV variability interactions do not depend on the *R* signal

Using the same logic exploited in the analysis of closed loop CV variability interactions, the information transfer along the pressure-to-flow pathway, namely from MAP to MCBv, and along the reverse causal pathway describing the Cushing reflex and responses to an increase of intracranial pressure, namely from MCBv to MAP, was assessed without accounting for *R* as confounding factor and by conditioning out RCM and CAP. Findings allowed us to elucidate the impact of *R* and the type of *R* on the evaluation of closed loop CBV variability interactions. Tests on surrogate data stressed that meaningful CBV variability interactions are present in most of subjects regardless of the experimental condition, groups and strategy adopted to account for *R* (i.e. TE types).

Remarkably, differently from CV analysis, results of TE did not depend on conditioning on *R* given that unconditional and conditional TEs were similar. Moreover, conditional TEs from MAP to MCBv, did not vary across either group or experimental condition. This conclusion did not depend on the type of *R* signal utilized to condition the pressure-to-flow relationship. This conclusion held even in the reverse causal direction, namely from MCBv to MAP along the flow-to-pressure pathway. The similar impact of RCM and CAP suggests that closed loop CBV variability interactions are similarly influenced by different aspects of *R*. RCM signal is usually considered to be a surrogate of the intrathoracic pressure inducing respiratory oscillations of MCBv, mediated by changes of intracranial pressure driven by respiratory movements of cerebrospinal fluid (Yildiz *et al* 2017, Porta *et al* 2022), and modifications of MAP as a consequence of the respiratory synchronization of right and left stroke volumes (Toska and Eriksen 1993, Caiani *et al* 2002, Elstad *et al* 2018). CAP was utilized in our study with the sole intention to test a *R* signal different from the RCM one but exhibiting a dominant component at the respiratory rate like *R*. Arterial pCO_2 could be an important confounding factor for the pressure-to-flow relationship given that alterations of arterial pCO_2 change MCBv regardless of MAP variations via modulations of cerebral autoregulation (Ogoh 2019). Unfortunately, CAP measured in this study is not arterial pCO_2. Only a value of CAP per respiratory cycle, taken at the end of expiration and commonly referred to as $etCO_2$, was considered an estimate of arterial pCO_2 (Panerai *et al* 1999b, Battisti-Charbonney *et al* 2011, Marmarelis *et al* 2020). Therefore, it is not surprising to find out that the respiratory component of CAP has a limited impact CBV causality analysis.

4.5. Abnormal CV response to STAND in POTS

The usual autonomic responses to an orthostatic stressor were observed, with POTS having a stronger sympathetic activation. During STAND, the expected vagal reduction (Pomeranz *et al* 1985) was evident in both groups, as suggested by the significant decrease of μ_{HP}. STAND induces a sympathetic activation in healthy subjects resulting in greater values of the LF_{SAP} power (Cooke *et al* 1999, Marchi *et al* 2016a). In this study a greater LF_{SAP} power increase was detected in POTS during STAND compared to CONTROL, thus confirming the abnormal sympathetic response to the gravitational stimulus typical of the pathology (Furlan *et al* 1998, Raj 2013).

It has been reported that the information genuinely transferred from SAP to HP conditioned on RCM increased during a postural challenge in healthy subjects (Porta *et al* 2011, Faes *et al* 2013a, Porta *et al* 2015, Bari *et al* 2017). This increment indicates the strong involvement of the baroreflex in counteracting the decrease of venous return associated with the orthostatic stimulus. This study confirmed previous findings in the CONTROL group. Since the expected increase of the genuine information transferred from SAP to HP during STAND was not detected in POTS, this missing response suggests a baroreflex impairment in this population. Interestingly, a similar absent response to orthostatic challenge was reported in Bari *et al* (2017) in a population with recurrent postural syncope.

Remarkably, in the reverse causal direction from HP to SAP, we observed a decrease of the information transfer conditioned on RCM. This observation confirmed that postural challenge inverts the direction of the information flow in the HP-SAP closed loop compared to REST, as suggested in Porta *et al* (2011) using a directionality index assessing the balance between information flows along the two opposite pathways of the HP-SAP closed loop.

4.6. Normal CBV response STAND in POTS

We confirmed that orthostatic challenge induced a decrease of μ_{MCBV} (Carey *et al* 2001, Bari *et al* 2017, Wells *et al* 2020, Gelpi *et al* 2022a). This result is the likely consequence of the sympathetic activation associated to STAND increasing CBV resistance. However, the decline of μ_{MCBV} does not necessarily indicate an impairment of cerebral autoregulation as suggested under head-up tilt in healthy individuals (Carey *et al* 2001, Gelpi *et al* 2022a). Remarkably, this finding was observed in both CONTROL and POTS, and it could not be attributed to modifications of arterial pCO_2 given that $etCO_2$ did not vary with STAND in both groups. However, during STAND, the variability of MCBv at the *R* rate in POTS was higher than that in CONTROL. This finding is more likely to be the consequence of the greater contribution of MAP variability in the same frequency band in POTS

than in CONTROL more than the effect of dysregulation of cerebral autoregulation, modifying the sensitivity of pressure-to-flow relationship (Zhang *et al* 1998) or changing $etCO_2$ (Panerai *et al* 1999b), given that both markers were similar across the two groups.

In the presence of an impairment of the CBV regulatory mechanisms, we would expect an increase of the TE from MAP to MCBv during STAND (Bari *et al* 2017). In the present study, the TE from MAP to MCBv did not vary with STAND regardless of the strategy adopted with *R*. This result was observed in both populations, thus indicating a preservation of CBV control mechanism in POTS individuals. This result suggests that the observed sympathetic overactivation of POTS, supported by the greater values of the LF_{SAP} power in POTS compared to CONTROL during STAND, did not necessarily lead to an impairment of cerebral autoregulation.

The preservation of the CBV control is supported by the invariance of the TE from MCBv to MAP across groups and experimental conditions (Bari *et al* 2017, Saleem *et al* 2018, Bari *et al* 2021) and the steadiness of $etCO_2$ in this experimental protocol, thus indicating even the maintenance of Cushing-like reflexes (Cushing 1902, McBryde *et al* 2017) responsible for continuous corrections MAP when MCBv assumes inappropriate values.

4.7. Limitations of the study and future developments

REST was taken while sitting, thus limiting comparison with previous studies assessing basal CV and CBV dynamic interactions in the supine position (Porta *et al* 2015, Gelpi *et al* 2022a). However, if the baseline condition was at supine resting, responses to the postural challenge would be greater than those observed in the present study, thus suggesting that the observed impairment of the baroreflex in POTS is detectable with an orthostatic stressor of limited intensity. Conversely, the preservation of CBV control observed in this study might not be confirmed in the case of an orthostatic challenge of greater intensity. The missing variable in the present experimental protocol is the direct measurement of sympathetic activity to assess the degree of activation of the adrenergic system (Pagani *et al* 1997, Cooke *et al* 1999, Hart *et al* 2010) and to compute the information transfer along the sympathetic arm of the baroreflex (Marchi *et al* 2016b) in addition to that along the cardiac arm assessed in this study. The results of this study might be impacted by the pharmacological therapy of POTS that reduced chronically the degree of sympathetic activation in our POTS group but did not prevent POTS individuals from being more tachycardic than CONTROL subjects at REST. MCBF was approximated with MCBv. However, MCBv could be considered a proxy of MCBF exclusively under the hypothesis of steadiness of vessel diameter (Aaslid *et al* 1982). This study did not check whether this hypothesis held even though previous studies observed negligible modifications of cerebral artery diameter in response to moderate changes of MAP and at values of $etCO_2$ measured in the present study (Giller *et al* 1993, Coverdale *et al* 2014, Verbree *et al* 2014). RCM signal has a smoother morphology related to the inertia of the chest, while CAP indicates much more evidently the onset of the respiratory cycle with sudden variations between inspiratory and expiratory pCO_2. Different morphology and phase shift between RCM and CAP signals in relation to similar setting of the analysis might have played a role on the conclusions. Future studies should investigate deeply these factors. Our preliminary results suggest that making smoother the CAP by filtering it, while preserving the frequency content from 0 to 0.5 Hz, does not modify conclusions of this study. Surrogate analysis highlighted the significant presence of interactions between CV and CBV variability series in both causal directions, thus suggesting the possibility of enlarging the application to clinical settings. However, future developments should be focused on reducing dispersion of indexes that might be related to methodological issues, thus increasing the statistical power of the analysis. Future studies should check whether phase lead of MCBv to MAP (Zhang *et al* 1998), that does not necessarily indicate a causal relationship from MCBv to MAP, might have contributed to the relevance of the flow-to-pressure pathway detected in this study by analyzing the relationship between phase lead and causality markers, even from a theoretical standpoint. Given the dependence of cerebral autoregulation on $etCO_2$ (Ogoh 2019), future studies should consider conditioning out etCO2 (Saleem *et al* 2018). In the present study the effect of conditioning TE on $etCO_2$ is expected to be limited given that μ_{etCO2} did not vary, the variability of $etCO_2$ was very small and did not exhibit specific rhythm in the VLF and LF bands.

5. Conclusions

The study assessed causal CV and CBV variability interactions in POTS individuals experiencing an exaggerated sympathetic activation during orthostatic challenge. Causality was assessed via TE without conditioning out *R* and after accounting for *R* signal as a confounding factor. Two different *R* signals were considered, namely RCM and CAP, both exhibiting dominant oscillations at the respiratory rate. The study stresses the relevance of accounting for *R* when assessing CV control and suggests that this conclusion might depend on the type of selected *R* signal with RCM more impactful on the analysis than CAP likely because CAP is less informative about inputs capable to drive HP changes at the respiratory rate independent of modifications of SAP compared

to RCM. The impact of R was negligible over CBV dynamic interactions likely because direct influences of R on MAP and MCBv dynamics are irrelevant and respiratory components observed in MAP and MCBv variability series are transmitted through their dynamic interactions.

Data availability statement

The data cannot be made publicly available upon publication because they contain sensitive personal information. The data that support the findings of this study are available upon reasonable request from the authors.

Author contributions

FG and AP conceived and designed the research; RW performed experiments; FG analyzed the data; FG and AP drafted the manuscript; FG and AP prepared the figures; FG, VB, BC, BDM, RW, MB, and AP interpreted the results; FG, VB, BC, BDM, RW, MB, and AP edited and revised the manuscript; FG, VB, BC, BDM, RW, MB., and AP approved the final version of the manuscript.

Funding

No specific support was received for this research.

Conflict of interest

The authors declare that the research was conducted in the absence of any commercial or financial relationships that could be construed as a potential conflict of interest.

ORCID iDs

Francesca Gelpi https://orcid.org/0000-0002-9221-6153
Mathias Baumert https://orcid.org/0000-0003-2984-2167
Alberto Porta https://orcid.org/0000-0002-6720-9824

References

Aaslid R, Markwalder T M and Nornes H 1982 Noninvasive transcranial doppler ultrasound recording of flow velocity in basal cerebral arteries *J. Neurosurg.* **57** 769–74

Abreu R M, Catai A M, Cairo B, Rehder-Santos P, Silva C D, De Favari Signini E, Sakaguchi C A and Porta A 2020 A transfer entropy approach for the assessment of the impact of inspiratory muscle training on the cardiorespiratory coupling of amateur cyclists *Front. Physiol.* **11** 134

Akaike H 1974 A new look at the statistical novel identification *IEEE Trans. Autom. Control* **19** 716–23

Andrzejak R G, Kraskov A, Stogbauer H, Mormann F and Kreuz T 2003 Bivariate surrogate techniques: necessity, strengths, and caveats *Phys. Rev. E Stat. Nonlin. Soft. Matter. Phys.* **68** 066202

Barbic F, Minonzio M, Cairo B, Shiffer D, Zamuner A R, Cavalieri S, Dipaola F, Magnavita N, Porta A and Furlan R 2020 Work ability assessment and its relationship with cardiovascular autonomic profile in postural orthostatic tachycardia syndrome *Int. J. Environ. Res Public Health* **17** 7836

Bari V, De Maria B, Mazzucco C E, Rossato G, Tonon D, Nollo G, Faes L and Porta A 2017 Cerebrovascular and cardiovascular variability interactions investigated through conditional joint transfer entropy in subjects prone to postural syncope *Physiol. Meas.* **38** 976–91

Bari V, Fantinato A, Vaini E, Gelpi F, Cairo B, De Maria B, Pistuddi V, Ranucci M and Porta A 2021 Impact of propofol general anesthesia on cardiovascular and cerebrovascular closed loop variability interactions *Biomed. Signal Process. Control* **68** 102735

Bari V, Marchi A, De Maria B, Rossato G, Nollo G, Faes L and Porta A 2016 Nonlinear effects of respiration on the crosstalk between cardiovascular and cerebrovascular control systems *Phil. Trans. R. Soc. A Math. Phys. Eng. Sci.* **374** 20150179

Barnett L, Barrett A B and Seth A K 2009 Granger causality and transfer entropy are equivalent for Gaussian variables *Phys. Rev. Lett.* **103** 238701

Baselli G, Cerutti S, Badilini F, Biancardi L, Porta A, Pagani M, Lombardi F, Rimoldi O, Furlan R and Malliani A 1994 Model for the assessment of heart period and arterial pressure variability interactions and of respiration influences *Med. Biol. Eng. Comput.* **32** 143–52

Baselli G, Porta A, Rimoldi O, Pagani M and Cerutti S 1997 Spectral decomposition in multichannel recordings based on multivariate parametric identification *IEEE Trans. Biomed. Eng.* **44** 1092–101

Battisti-Charbonney A, Fisher J and Duffin J 2011 The cerebrovascular response to carbon dioxide in humans *J. Physiol.* **589** 3039–48

Caiani E G, Turiel M, Muzzupappa S, Colombo L P, Porta A and Baselli G 2002 Noninvasive quantification of respiratory modulation on left ventricular size and stroke volume *Physiol. Meas.* **23** 567–80

Carey B J, Manktelow B N, Panerai R B and Potter J F 2001 Cerebral autoregulatory responses to head-up tilt in normal subjects and patients with recurrent vasovagal syncope *Circulation* **104** 898–902
Claassen J A H R, Meel-van den Abeelen A S S, Simpson D M and Panerai R B 2016 on behalf of the international cerebral autoregulation research network (CARNet) Transfer function analysis of dynamic cerebral autoregulation: a white paper from the international cerebral autoregulation research network *J. Cereb. Blood Flow Metab.* **36** 665–80
Cooke W H, Hoag J B, Crossman A A, Kuusela T A, Tahvanainen K U O and Eckberg D L 1999 Human responses to upright tilt: a window on central autonomic integration *J. Physiol.* **517** 617–28
Corbier C, Chouchou F, Roche F, Barthélémy J-C and Pichot V 2020 Causal analyses to study autonomic regulation during acute head-out water immersion, head-down tilt and supine position *Exp. Physiol.* **105** 1216–22
Coverdale N S, Gati J S, Opalevych O, Perrotta A and Shoemaker J K 2014 Cerebral blood flow velocity underestimates cerebral blood flow during modest hypercapnia and hypocapnia *J. Appl. Physiol.* **117** 1090–6
Cushing H 1902 Some experimental and clinical observations concerning states of increased intracranial tension *Am. J. Med. Sci.* **124** 375–400
De Boer R W, Karemaker J M and Strackee J 1987 Hemodynamic fluctuations and baroreflex sensitivity in humans: a beat-to-beat model *Am. J. Physiol.* **253** H680–9
Eckberg D L 2003 The human respiratory gate *J. Physiol.* **548** 339–52
Elstad M, O'Callaghan E L, Smith A J, Ben-Tal A and Ramchandra R 2018 Cardiorespiratory interactions in humans and animals: rhythms for life *Am. J. Physiol.* **315** H6–17
Faes L, Nollo G and Porta A 2013a Mechanisms of causal interaction between short-term RR interval and systolic arterial pressure oscillations during orthostatic challenge *J. Appl. Physiol.* **114** 1657–67
Faes L, Porta A, Rossato G, Adami A, Tonon D, Corica A and Nollo G 2013b Investigating the mechanisms of cardiovascular and cerebrovascular regulation in orthostatic syncope through an information decomposition strategy *Auton. Neurosci.: Basic Clin.* **178** 76–82
Farquhar W B, Taylor J A, Darling S E, Chase K P and Freeman R 2000 Abnormal baroreflex responses in patients with idiopathic orthostatic intolerance *Circulation* **102** 3086–91
Furlan R, Jacob G, Snell M, Robertson D, Porta A, Harris P and Mosqueda-Garcia R 1998 Chronic orthostatic intolerance: a disorder with discordant cardiac and vascular sympathetic control *Circulation* **98** 2154–9
Gelpi F, Bari V, Cairo B, De Maria B, Tonon D, Rossato G, Faes L and Porta A 2022a Dynamic cerebrovascular autoregulation in patients prone to postural syncope: comparison of techniques assessing the autoregulation index from spontaneous variability series *Auton. Neurosci.: Basic Clin.* **237** 102920
Gelpi F, Bari V, Cairo B, De Maria B, Wells R, Baumert M and Porta A 2022b Cardiovascular and cerebrovascular information transfer might depend on the type of conditioning respiratory signal *12th Conf. European Study Group on Cardiovascular Oscillations (ESGCO) (Štrbské Pleso, Slovakia, 9–12 October 2022)* (IEEE press) (https://doi.org/10.1109/ESGCO55423.2022.9931377)
Giller C A, Bowman G, Dyer H, Mootz L and Krippner W 1993 Cerebral arterial diameters during changes in blood pressure and carbon dioxide during craniotomy *Neurosurgery* **32** 737–41
Granger C W J 1980 Testing for causality. A personal viewpoint *J. Econ. Dyn. Control* **2** 329–52
Hart E C, Joyner M J, Wallin B G, Karlsson T, Curry T B and Charkoudian N 2010 Baroreflex control of muscle sympathetic nerve activity: a nonpharmacological measure of baroreflex sensitivity *Am. J. Physiol.* **298** H816–22
Joshi B, Brady K, Lee J, Easley B, Panigrahi R, Smielewski P, Czosnyka M and Hogue C W 2010 Impaired autoregulation of cerebral blood flow during rewarming from hypothermic cardiopulmonary bypass and its potential association with stroke *Anesth. Analg.* **110** 321–8
Laude D *et al* 2004 Comparison of various techniques used to estimate spontaneous baroreflex sensitivity (the EuroBaVar study) *Am. J. Physiol.* **286** R226–31
Marchi A, Bari V, De Maria B, Esler M, Lambert E, Baumert M and Porta A 2016a Calibrated variability of muscle sympathetic nerve activity during graded head-up tilt in humans and its link with noradrenaline data and cardiovascular rhythms *Am. J. Physiol.* **310** R1134–43
Marchi A, Bari V, De Maria B, Esler M, Lambert E, Baumert M and Porta A 2016b Simultaneous characterization of sympathetic and cardiac arms of the baroreflex through sequence techniques during incremental head-up tilt *Front. Physiol.* **7** 438
Marmarelis V Z, Shin D C, Oesterreich M and Mueller M 2020 Quantification of dynamic cerebral autoregulation and CO2 dynamic vasomotor reactivity impairment in essential hypertension *J. Appl. Physiol.* **128** 397–409
McBryde F D, Malpas S C and Paton J F 2017 Intracranial mechanisms for preserving brain blood flow in health and disease *Acta Physiol.* **219** 274–87
Muenter Swift N, Charkoudian N, Dotson R M, Suarez G A and Low P A 2005 Baroreflex control of muscle sympathetic nerve activity in postural orthostatic tachycardia syndrome *Am. J. Physiol.* **289** H1226–33
Nakagawa K, Serrador J M, LaRose S L and Sorond F A 2011 Dynamic cerebral autoregulation after intracerebral hemorrhage: a case-control study *BMC Neurol.* **11** 108
Ogoh S 2019 Interaction between the respiratory system and cerebral blood flow regulation *J. Appl. Physiol.* **127** 1197–205
Otite F *et al* 2014 Impaired cerebral autoregulation is associated with vasospasm and delayed cerebral ischemia in subarachnoid hemorrhage *Stroke* **45** 677–82
Pagani M, Montano N, Porta A, Malliani A, Abboud F M, Birkett C and Somers V K 1997 Relationship between spectral components of cardiovascular variabilities and direct measures of muscle sympathetic nerve activity in humans *Circulation* **95** 1441–8
Panerai R B, Dawson S L and Potter J F 1999a Linear and nonlinear analysis of human dynamic cerebral autoregulation *Am. J. Physiol.* **277** H1089–99
Panerai R B, Deverson S T, Mahony P, Hayes P and Evans D H 1999b Effects of CO_2 on dynamic cerebral autoregulation measurement *Physiol. Meas.* **20** 265–75
Pinna G D, Porta A, Maestri R, De Maria B, Dalla Vecchia L A and La Rovere M T 2017 Different estimation methods of spontaneous baroreflex sensitivity have different predictive value in heart failure patients *J. Hypertens.* **35** 1666–75
Pomeranz B *et al* 1985 Assessment of autonomic function in humans by heart rate spectral analysis *Am. J. Physiol.* **248** H151–3
Porta A, Bari V, Bassani T, Marchi A, Pistuddi V and Ranucci M 2013a Model-based causal closed loop approach to the estimate of baroreflex sensitivity during propofol anesthesia in patients undergoing coronary artery bypass graft *J. Appl. Physiol.* **115** 1032–42
Porta A, Bari V, De Maria B, Takahashi A C M, Guzzetti S, Colombo R, Catai A M, Raimondi F and Faes L 2017 Quantifying net synergy/redundancy of spontaneous variability regulation via predictability and transfer entropy decomposition frameworks *IEEE Trans. Biomed. Eng.* **64** 2628–38
Porta A, Baselli G, Rimoldi O, Malliani A and Pagani M 2000 Assessing baroreflex gain from spontaneous variability in conscious dogs: Role of causality and respiration *Am. J. Physiol.* **279** H2558–67

Porta A, Bassani T, Bari V, Pinna G D, Maestri R and Guzzetti S 2012 Accounting for respiration is necessary to reliably infer Granger causality from cardiovascular variability series *IEEE Trans. Biomed. Eng.* **59** 832–41
Porta A, Castiglioni P, Di Rienzo M, Bassani T, Bari V, Faes L, Nollo G, Cividjan A and Quintin L 2013b Cardiovascular control and time domain Granger causality: insights from selective autonomic blockade *Phil. Trans. R. Soc. A Math. Phys. Eng. Sci.* **371** 20120161
Porta A, Catai A M, Takahashi A C M, Magagnin V, Bassani T, Tobaldini E, van de Borne P and Montano N 2011 Causal relationships between heart period and systolic arterial pressure during graded head-up tilt *Am. J. Physiol.* **300** R378–86
Porta A and Faes L 2016 Wiener-Granger causality in network physiology with applications to cardiovascular control and neuroscience *Proc. IEEE* **104** 282–309
Porta A, Faes L, Nollo G, Bari V, Marchi A, De Maria B, Takahashi A C M and Catai A M 2015 Conditional self-entropy and conditional joint transfer entropy in heart period variability during graded postural challenge *PLoS One* **10** e0132851
Porta A, Gelpi F, Bari V, Cairo B, De Maria B, Tonon D, Rossato G, Ranucci M and Faes L 2022 Categorizing the role of respiration in cardiovascular and cerebrovascular variability interactions *IEEE Trans. Biomed. Eng.* **69** 2065–76
Raj S R 2013 Postural tachycardia syndrome (POTS) *Circulation* **127** 2336–42
Saleem S, Teal P D, Howe C A, Tymko M M, Ainslie P N and Tzeng Y-C 2018 Is the Cushing mechanism a dynamic blood pressure-stabilizing system? Insights from Granger causality analysis of spontaneous blood pressure and cerebral blood flow *Am. J. Physiol.* **315** R484–95
Schreiber T 2000 Measuring information transfer *Phys. Rev. Lett.* **85** 461–4
Shankhwar V, Singh D and Deepak K K 2022 Cardiac-vascular-respiratory coupling analysis during 6-degree head-down tilt microgravity analogue *Biomed. Signal Process. Control* **72** 103358
Tarumi T, Dunsky D I, Khan M A, Liu J, Hill C, Armstrong K, Martin-Cook K, Cullum C M and Zhang R 2014 Dynamic cerebral autoregulation and tissue oxygenation in amnestic mild cognitive impairment *J. Alzheimer's Dis.* **41** 765–78
Task Force of the European Society of Cardiology and the North American Society of Pacing and Electrophysiology 1996 Heart rate variability: standards of measurement, physiological interpretation and clinical use *Circulation* **93** 1043–65
Taylor J A and Eckberg D L 1996 Fundamental relations between short-term RR interval and arterial pressure oscillations in humans *Circulation* **93** 1527–32
Tiecks F P, Lam A M, Aaslid R and Newell D W 1995 Comparison of static and dynamic cerebral autoregulation measurements *Stroke* **26** 1014–9
Toska K and Eriksen M 1993 Respiration-synchronous fluctuations in stroke volume, heart rate and arterial pressure in humans *J. Physiol.* **472** 501–12
Tzeng Y C, MacRae B A, Ainslie P N and Chan G S H 2014 Fundamental relationships between blood pressure and cerebral blood flow in humans *J. Appl. Physiol.* **117** 1037–48
Vaini E, Bari V, Fantinato A, Pistuddi V, Cairo B, De Maria B, Ranucci M and Porta A 2019 Causality analysis reveals the link between cerebrovascular control and acute kidney dysfunction after coronary artery bypass grafting *Physiol. Meas.* **40** 064006
Verbree J, Bronzwaer A-S G T, Ghariq E, Versluis M J, Daemen M J A P, van Buchem M A, Dahan A, van Lieshout J J and van Osch M J P 2014 Assessment of middle cerebral artery diameter during hypocapnia and hypercapnia in humans using ultra-high-field MRI *J. Appl. Physiol.* **117** 1084–9
Vicente R, Wibral M, Lindner M and Pipa G 2011 Transfer entropy–a model-free measure of effective connectivity for the neurosciences *J. Comput. Neurosci.* **30** 45–67
Wells R, Malik V, Brooks A G, Linz D, Elliott A D, Sanders P, Page A, Baumert M and Lau D H 2020 Cerebral blood flow and cognitive performance in postural tachycardia syndrome: insights from sustained cognitive stress test *J. Am. Heart Assoc.* **9** e017861
Yildiz S, Thyagaraj S, Jin N, Zhong X, Heidari Pahlavian S, Martin B A, Loth F, Oshinski J and Sabra K G 2017 Quantifying the influence of respiration and cardiac pulsations on cerebrospinal fluid dynamics using real-time phase-contrast MRI *J. Magn. Reason. Imaging* **46** 431–9
Zhang R, Zuckerman J H, Giller C A and Levine B D 1998 Transfer function analysis of dynamic cerebral autoregulation in humans *Am. J. Physiol.* **274** H233–41
Zhang R, Zuckerman J H, Iwasaki K, Wilson T E, Crandall C G and Levine B D 2002 Autonomic neural control of dynamic cerebral autoregulation in humans *Circulation* **106** 1814–20